JUL 23 1971

Bellcomm

955 L'Enfant Plaza North, S.W.
Washington, D. C. 20024

B71 06058

date: June 30, 1971

to: Distribution

from: S. L. Levie, Jr.

subject: Possible Effects of Mascon Disturbances on Apollo 15 Orbit Determination and Navigation - Case 310

ABSTRACT

The docked Apollo 15 spacecraft are to fly in a low lunar orbit for about nineteen hours prior to LM descent. This orbit will carry the spacecraft over the mascon basins Imbrium, Serenitatis, and Crisium, and near the Orientale mascon. The influence of the mascons, which are not modelled by the L1 lunar potential model, raises the possibility of large navigation errors prior to the landing. This study suggests that the major effect of the mascons will be an error in the orbital period, causing a downrange error of about 18,000 ft per revolution. Crossrange and altitude errors of some 5000 and 1000 ft due to mascons are in the same general range of magnitudes existing in the orbital determinations and predictions during the actual flight of the spacecraft in past missions.

Real time procedures for orbital navigation need not be changed because of the mascons. A DOI TRIM burn four revolutions before powered descent (PDI) seems unlikely. The LM downrange position correction at PDI (ΔRLS update via NOUN 69) should cope with downrange errors equally as well as it has in the past: crossrange errors remain the major uncorrectable error at PDI.

(NASA-CR-121357) POSSIBLE EFFECTS OF MASCON DISTURBANCES ON APOLLO 15 ORBIT DETERMINATION AND NAVIGATION (Bellcomm, Inc.) 30 p

N79-71921

Unclas
00/13 12099

FF No. 602

(PAGES) (CODE)

CR-121357

(NASA CR OR TMX OR AD NUMBER) (CATEGORY)

[redacted]

AUG 1971
RECEIVED
FACILITY
BRANCH

955 L'Enfant Plaza North, S.W.
Washington, D. C. 20024

B71 06058

date: June 30, 1971

to: Distribution

from: S. L. Levie, Jr.

subject: Possible Effects of Mascon Disturbances on Apollo 15 Orbit Determination and Navigation - Case 310

MEMORANDUM FOR FILE

INTRODUCTION

For a period of about nineteen hours, the docked Apollo 15 spacecraft will coast in a 60 nm by 8 nm lunar orbit which carries them directly over three large mascon basins: Imbrium, Serenitatis, and Crisium. Due to the considerable excess mass identified with these basins, there is natural concern as to the effects on orbit determination and prediction during the mission.

This paper reports a brief investigation into the kinds of problems that may be encountered due to unmodelled mascon disturbances. The investigation compared the effects of the L1 lunar gravitational potential model--to be used in the mission--against the effects of a simulated moon which adds mascons to the L1 model. The comparisons involved an L1 orbit determination and state propagation check, using simulated lunar data, and a study of orbit element and position error evolution over a nineteen hour period. The basic conclusion reached is that the possible errors introduced by the unmodelled mascons are significant, but that it appears that they may be compensated for.

TRAJECTORY FOR APOLLO 15

As a first in the Apollo series, the Apollo 15 lunar orbit will have a large selenographic inclination (about 26°) and a large selenographic node (about 107°). These values are required in order to achieve a landing at the Hadley-Apennines site, located at 26°.07 N, 3°.65 E. With respect to surface features, the trajectory will pass over the maria Crisium, Serenitatis, and Imbrium, and it

will pass just west of Mare Orientale. The 60 nm by 8 nm altitude trajectory preceding LM descent has its pericenter near the eastern edge of Mare Serenitatis. The docked spacecraft will be in this orbit for about nineteen hours. A state vector near the beginning of this period was taken from the Apollo 15 Operational Trajectory; it is given in selenocentric 1972 and selenocentric 1950 coordinates in Table 1.

LUNAR POTENTIAL MODELS

The L1 lunar potential model will be used for on-board and earth-based calculations for Apollo 15. Because this model represents averaged, or bulk, properties of the moon, it should not be expected to give the effects of local structures such as the mascon basins the spacecraft will fly over. On the other hand, there is no lunar potential model available which is confidently known to model the moon's potential in detail. Thus, for the purposes of this investigation, a detailed model had to be postulated which would simulate the moon adequately for a qualitative study.

The detailed model was obtained by adding to the L1 potential approximate potentials for the seven mascons listed in Table 2. This list contains the known mascons affecting Apollo 15. As Table 2 indicates, some of the mascons were represented as single point masses, while others were represented as a set of seven point masses.* All mass points were assigned a depth of 100 km below the mean lunar surface. The potentials of each of the point masses were expanded in spherical harmonics up to (7,7), scaled to the known lunar mass, and then added to the L1 potential, also scaled to the lunar mass. The resulting potential, given with the L1 potential in Table 3, has the correct lunar mass and a center of mass offset on the order of 500 feet relative to the selenographic origin. Its C_{20} and C_{22} values are slightly different from the currently accepted astronomical values.

Use of the potential in Table 3, which will be called the mascon potential, involves the following important assumptions:

---

*The sets of seven were arranged with one point at the basin's center and the other six in a hexagonal pattern centered on the first one.

1. Global effects for Apollo 15 may be represented by the L1 model.

2. All local effects for Apollo 15 may be represented by the point masses indicated in Table 2.

3. Truncation of the model at (7,7) will not delete effects important for a qualitative study.

4. The center of mass offset and the C_{20} and C_{22} offsets are probably within the astronomical uncertainties of these values and will not contribute significantly to a qualitative study.

ORBIT DETERMINATION - PDI TARGETING

The state vector of Table 1 was used with the mascon potential to generate three full frontside passes of simulated doppler tracking data. The L1 potential then was used with the first pass data in a least squares regression. Finally, the solution state was propagated forward three revolutions under the L1 potential, and predicted doppler data were generated. The differences (residuals) between the simulated and predicted doppler data were computed and plotted as Figure 1. The figure shows that the residuals seem "small"* in the regression zone, but their growth in the propagation zone shows that simple propagation of an L1-determined state vector in an L1 potential field can lead to a strong divergence of the L1 and actual data.

The meaning of the residuals in the regression zone was explored by computing the UVW coordinates of the solution state (propagated with the L1 potential) relative to the supposed true position of the spacecraft moving in the mascon potential.**The result was that--in the

---

*These residuals are still two or three times larger than is customary when using the L1 potential in real time Apollo work.

**A UVW frame is a time-varying frame in which U points along the instantaneous radius vector, V points in the instantaneous downrange direction and normal to U, and W completes the righthanded triad, pointing in the instantaneous crosstrack direction. The UVW frame was computed for the spacecraft moving in the mascon potential field, and the relative position of the spacecraft moving in the L1 potential field was decomposed into this frame.

regression zone--the L1-predicted position had an average downrange offset of about 1200 ft, a cross track error varying from zero to 3500 ft and back to zero, and a vertical error varying from 2000 ft to zero and back to 2000 ft. Downrange error grows at an average rate of 18,000 ft per resolution. Crossrange and altitude error continue to oscillate sinusoidally to about the same extremes.

The "N69 ΔRLS" update at powered descent is quite capable of correcting this downrange error. Additionally, procedures exist for including systematic propagation errors in all three directions in the state vector at descent, using the experience gained during the revolutions between DOI and PDI. The non-systematic crossrange error remains the major uncorrectable error at PDI. MSC's estimate of 7000 ft 1σ appears appropriate and inclusive of mascon effects. Use of landmark tracking should improve the situation further.

ORBIT EVOLUTION - DOI TARGETING

The initial state vector in Table 1 was integrated forward nineteen hours assuming the L1 lunar potential model. This was repeated using the mascon potential model. Figures 2 through 13 show the selenographic elements* a, e, i, ω, Ω, and M for each potential and the moment-by-moment differences between the elements for the two potential models. Note that the plots of element differences always show "mascon" minus "L1". Figures 14, 15, and 16 document the perilune altitude evolution for the two models. The UVW coordinates of the "L1 spacecraft" relative to the "mascon spacecraft" are presented as functions of time in Figures 17, 18, and 19.

All the graphs in Figures 2 through 19 share two major characteristics: they have long period trends and short period fine structure. The differing effects of the two potentials are manifested in the element difference curves. These curves show that small time scale element differences, as well as long time scale element rate differences, are generated by the mascon potential. The only exception is the semi-major axis, which has the same long period rate under the two potentials (i.e., no trend in Figure 2).

---

*Actually, it is element minus initial value that is plotted. The node, Ω, is referenced to the inertial frame selenocentric 1950.

The differences between semi-major axes and eccentricities (Figures 2 through 5) cause differences in the perilune altitudes (Figures 14, 15, and 16) for the two potentials which, after nineteen hours are less than about 1500 ft. The short term altitude differences (Figure 17) are always less than about a mile. Furthermore, the long term rate of decrease of perilune altitude (for either model) is about 400 ft/hr. Thus, there is no reasonable threat of crashing due to unmodelled mascon influences.

The major perturbations caused by the assumed mascon potential seem to be in the geometrical elements: inclination, node, argument of perilune, and mean anomaly. After nineteen hours this potential causes $\Delta i \sim 0\overset{\circ}{.}015$, $\Delta\Omega \sim -0.1°$, $\Delta\omega \sim 3°$, and $\Delta M \sim -1°$. The combined shift in argument of perilune and mean anomaly is clearly dominant, suggesting that downrange errors will be the principal effect of neglecting the mascon effects. This means that in each revolution the L1 potential would increment the lag error in its estimate of spacecraft position by about 24,000 ft. This rough conclusion is verified by Figure 18, which plots the downrange position of the "L1 spacecraft" relative to the actual spacecraft position in the mascon environment.

The crosstrack errors are sensitive to the somewhat cancelling effects of the inclination and node trends. This is evident from Figure 19, which shows the crosstrack position of the "L1 spacecraft" relative to the "mascon spacecraft." This curve, which is actually the crosstrack error curve, may be approximated as a sine wave with amplitude linearly growing in time and with a small, time-varying phase angle.

The DOI TRIM burn two revolutions before powered descent initiation is made only if the crosstrack error is over 50,000 ft, or if the altitude is outside the 30-70,000 ft range. It appears that mascons by themselves will not cause the burn to be necessary.

PERSPECTIVE

To assess the validity of the results just presented, two checks were made. The first used the customary L1 coefficients in the low order part of the mascon potential, to determine what portion of the potential produced the observed effects. It was found that the non-L1 contributions

(the high order coefficients) from the mascons were dominant. The second test used an Apollo 14 orbit in the same way that the Apollo 15 orbit was used in the preceding sections. The result was that the mascon effects on the Apollo 14 state were much weaker than on the Apollo 15 state. All errors grew from zero (little or no initial bias), and the downrange error growth rate was only about 4000 ft/rev.

CONCLUSIONS

Using an Apollo 15 Operational Trajectory state vector valid near the beginning of the nineteen hour coasting period prior to LM descent, pseudo doppler tracking data were generated assuming a mascon-laden moon. The L1 potential model was used in fitting this data over one front side pass and in propagating the solution state vector forward three revolutions. It appears that the doppler residuals in the fit zone are not as small as they were on past missions, and that they grow very large even one revolution past the fit zone. Techniques exist, however, to cope with them at PDI, except for the non-systematic crossrange errors.

The long term propagation tests carried out with the two potentials give a better perspective on this conclusion. Specifically, the principal long term error introduced by the assumed mascon distribution is apparently concentrated in the downrange direction, with about 18,000 ft/rev lag in the L1-predicted position. The short term effects of the mascons seem to be predominantly vertical accelerations, which are inconsequential for the 60 nm x 8 nm orbit of Apollo 15, and the long term effects seem to be due predominantly to horizontal accelerations. The horizontal accelerations lead to the downrange errors just mentioned. The DOI TRIM burn at PDI minus two revolutions is required if altitude or crosstrack errors are large, and is not affected by downrange errors. It appears that the mascons, by themselves, do not have sufficient effect to make the burn necessary.

Sterling Levie Jr.

2014-SLL-ksc

S. L. Levie, Jr.

Attachments
Tables 1-3
Figures 1-19

Table 1

APOLLO 15 STATE VECTOR
NEAR THE START OF THE NINETEEN
HOUR PRE-DESCENT COAST PERIOD

EPOCH: 30.0548611 July, 1971

COMPONENT	SELENOCENTRIC VALUE (ft and ft/sec)	
	1972	1950
X	4.3326961×10^6	4.3481024×10^6
Y	1.853519×10^6	1.8331466×10^6
Z	3.3147501×10^6	3.3305894×10^6
$\dot{X}$	3410.7142	3388.4905
$\dot{Y}$	-3744.0252	-3759.9817
$\dot{Z}$	-2257.3900	-2264.3267

Table 2

MASCON DATA* USED IN CONSTRUCTING
THE MASCON POTENTIAL MODEL

MASCON	MASS (μ moon)	CENTER (LAT, LONG)	REPRESENTATION (# MASS POINTS, DEPTH)
• Imbrium	27	(38°, -18°)	(7 , 100 km)
• Serenitatis	23	(28, 18°)	(7 , 100 km)
• Crisium	9.3	(16°, 58°)	(7 , 100 km)
• Orientale	4.6	(-20°, -95°)	(1 , 100 km)
Nectaris	8	(-16°, 34°)	(7 , 100 km)
Aestuum	10	(10°, - 8°)	(1 , 100 km)
Humorum	6.8	(-25°, -40°)	(1 , 100 km)
	89 TOTAL		

indicates Apollo 15 flies over or tangent to mascon.

---

*The data in this table are based on W. M. Kaula, "The Gravitational Field of the Moon," Science, 1969, and Wong, L., "Lunar Gravitational Model Derived from Doppler Data," presented at Spring AGU meeting, Washington, 1970.

Table 3

THE MASCON POTENTIAL COEFFICIENTS

The potential is assumed to have the form

$$V(r,\theta,\phi) = \frac{GM}{r} \sum_{\ell=0}^{\infty} \sum_{m=0}^{\ell} \left(\frac{r_o}{r}\right)^{\ell} P_\ell^m(\cos\theta)\,[C_{\ell m} \cos m\phi + S_{\ell m} \sin m\phi],$$

where (r,θ,ϕ) are spherical polar coordinates of a field point, P_ℓ^m is the associated Legendre function customarily used in Apollo, GM = 4.90278×10^3 km^3/sec^2 and r_o = 1738 km. Coefficients not listed below are zero. Numbers in parentheses are the coefficients for the L1 potential model. Mantissa-exponent format is used.

C_{00} = 1 (1)		
C_{10} = .2264-4	C_{11} = .6135-4	S_{11} = .1784-5
C_{20} = -.22262958-3 (-.207108-3)	C_{21} = .1771-4	S_{21} = .2491-5
	C_{22} = .28189157-4 (.20716-4)	S_{22} = .1689-5
C_{30} = .7028132-5 (.21-4)	C_{31} = .34089556-4 (.34-4)	S_{31} = -.1742-5
	C_{32} = .3172-5	S_{32} = .1938-6
	C_{33} = .3106702-5 (.2583-5)	S_{33} = .1768-6
C_{40} = -.8339-5	C_{41} = -.3582-5	S_{41} = -.1998-5
	C_{42} = .6292-6	S_{42} = -.4707-6
	C_{43} = .2970-6	S_{43} = -.6693-7
	C_{44} = .2081-7	S_{44} = -.2523-7

Table 3 (continued)

C_{50} = .3153-6	C_{51} = -.3395-5	S_{51} = .4870-6
	C_{52} = -.2353-6	S_{52} = -.2490-6
	C_{53} = .7003-7	S_{53} = -.4299-7
	C_{54} = .2273-7	S_{54} = -.8855-8
	C_{55} = -.6799-9	S_{55} = -.3731-8
C_{60} = .9006-5	C_{61} = -.6830-6	S_{61} = .8707-6
	C_{62} = -.2508-6	S_{62} = -.2942-7
	C_{63} = .3070-9	S_{63} = -.9627-8
	C_{64} = .2310-8	S_{64} = -.1878-8
	C_{65} = .2171-8	S_{65} = -.6372-9
	C_{66} = -.6362-10	S_{66} = -.6-65-10
C_{70} = .3364-5	C_{71} = .1218-5	S_{71} = .2367-6
	C_{72} = -.1050-6	S_{72} = .2795-7
	C_{73} = -.6631-8	S_{73} = -.1525-7
	C_{74} = -.4833-9	S_{74} = -.4405-9
	C_{75} = -.2824-9	S_{75} = .3188-10
	C_{76} = .1117-9	S_{76} = -.4201-10
	C_{77} = .2047-11	S_{77} = .3390-11

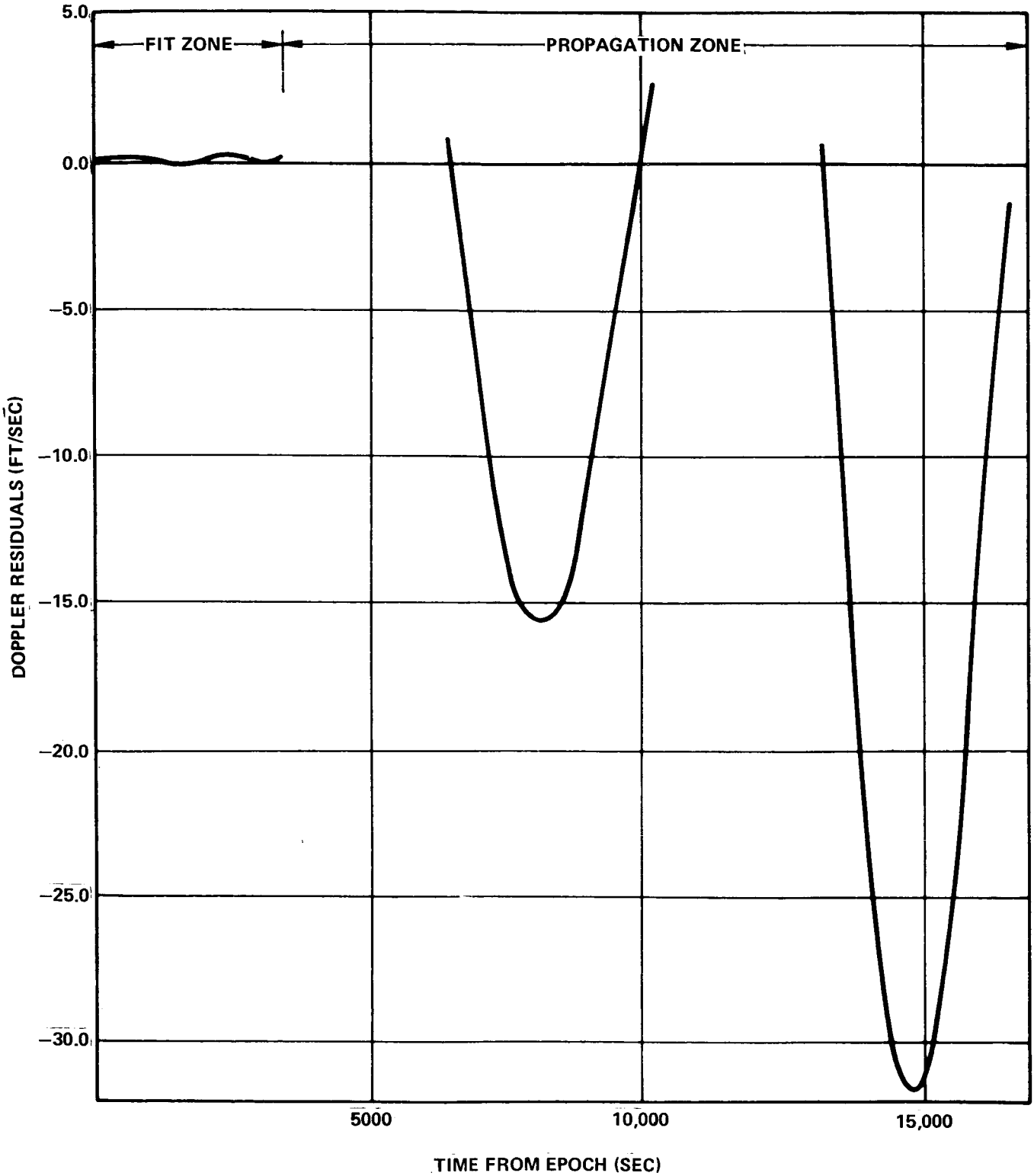

FIGURE 1 - DOPPLER DIFFERENCES BETWEEN SIMULATED MOON DATA AND L1 DATA

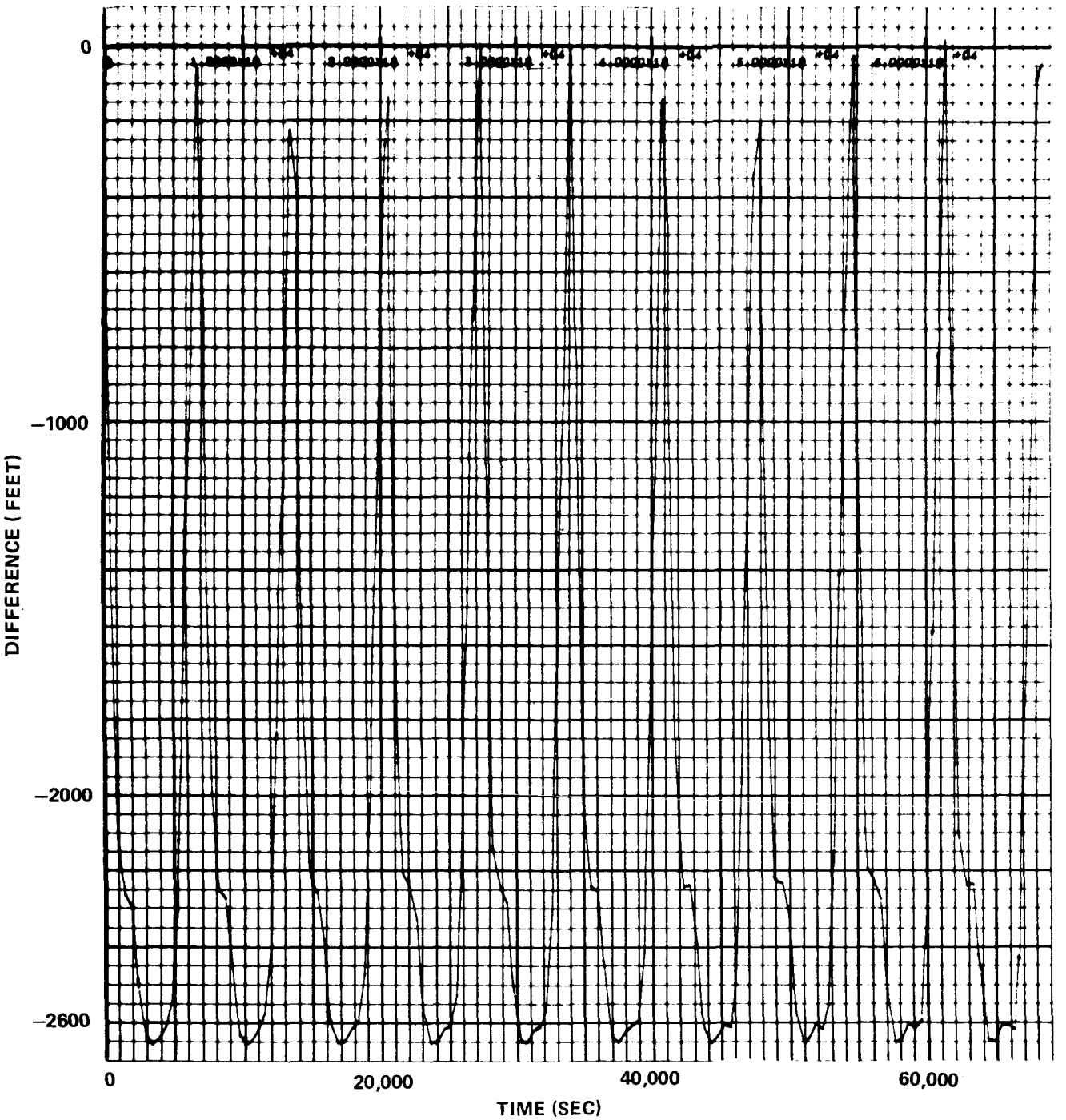

FIGURE 2 - SEMIMAJOR AXIS DIFFERENCES

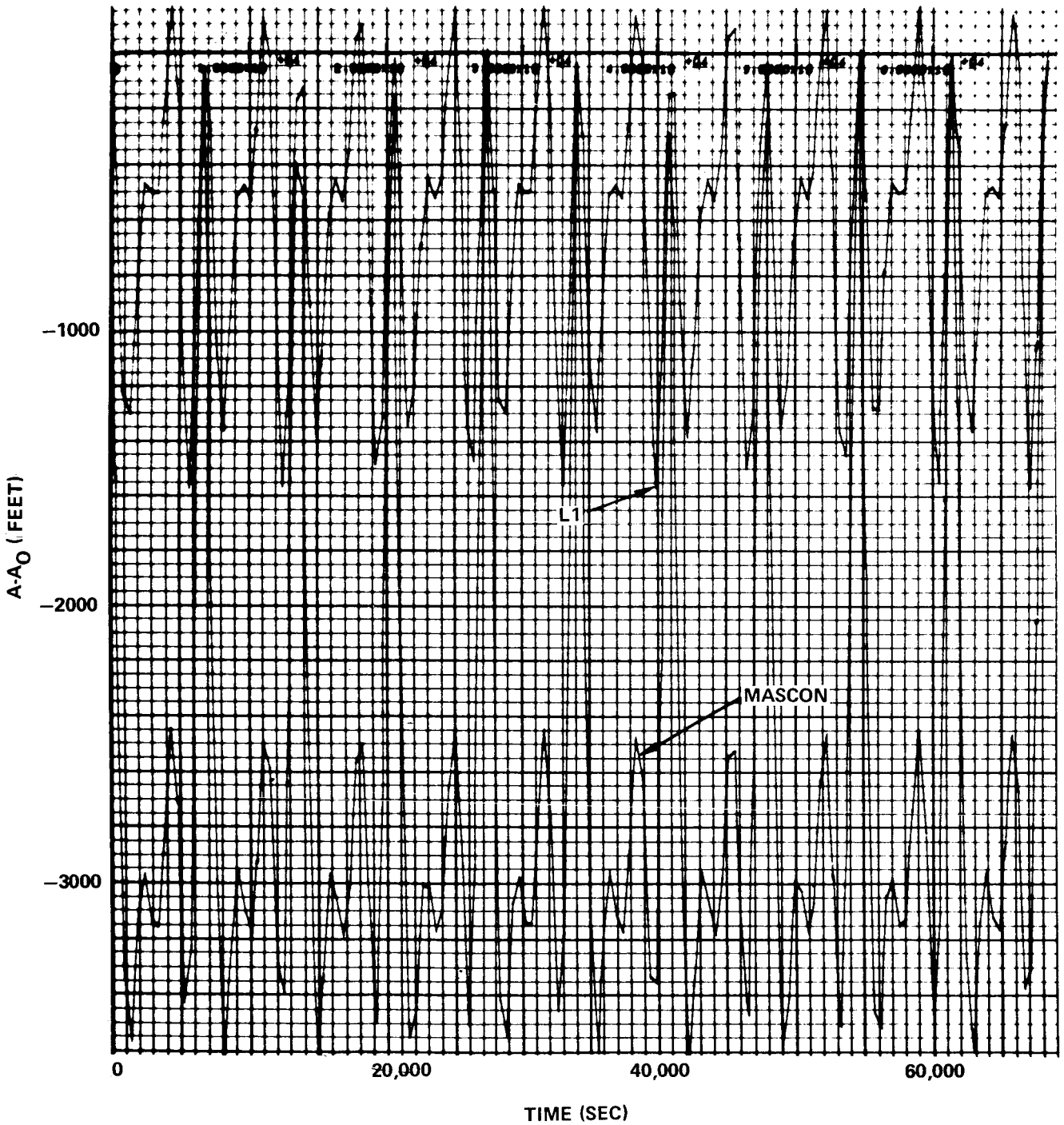

FIGURE 3 - SEMIMAJOR AXES [A_O = 5,898,049 FT.]

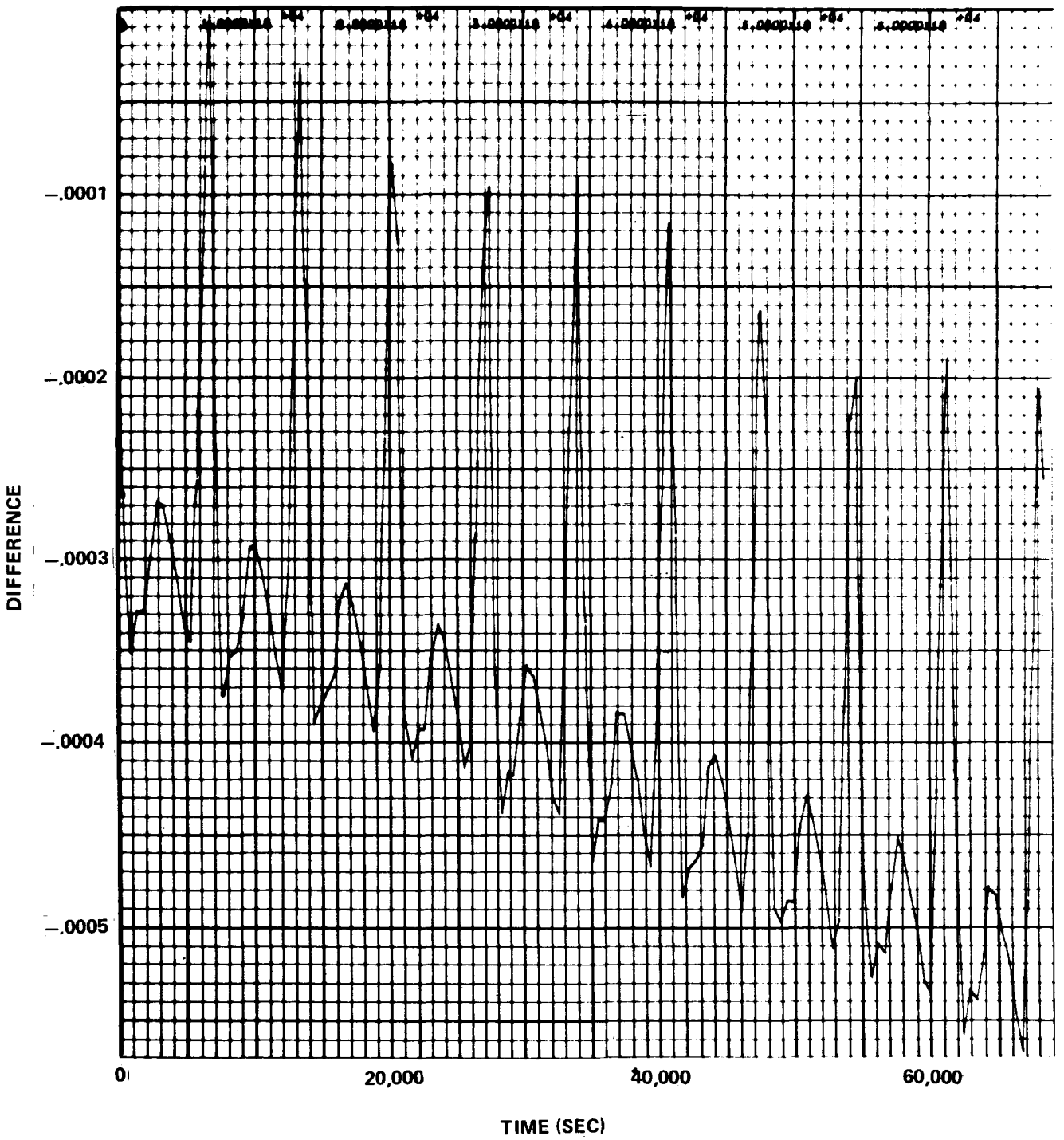

FIGURE 4 - ECCENTRICITY DIFFERENCES

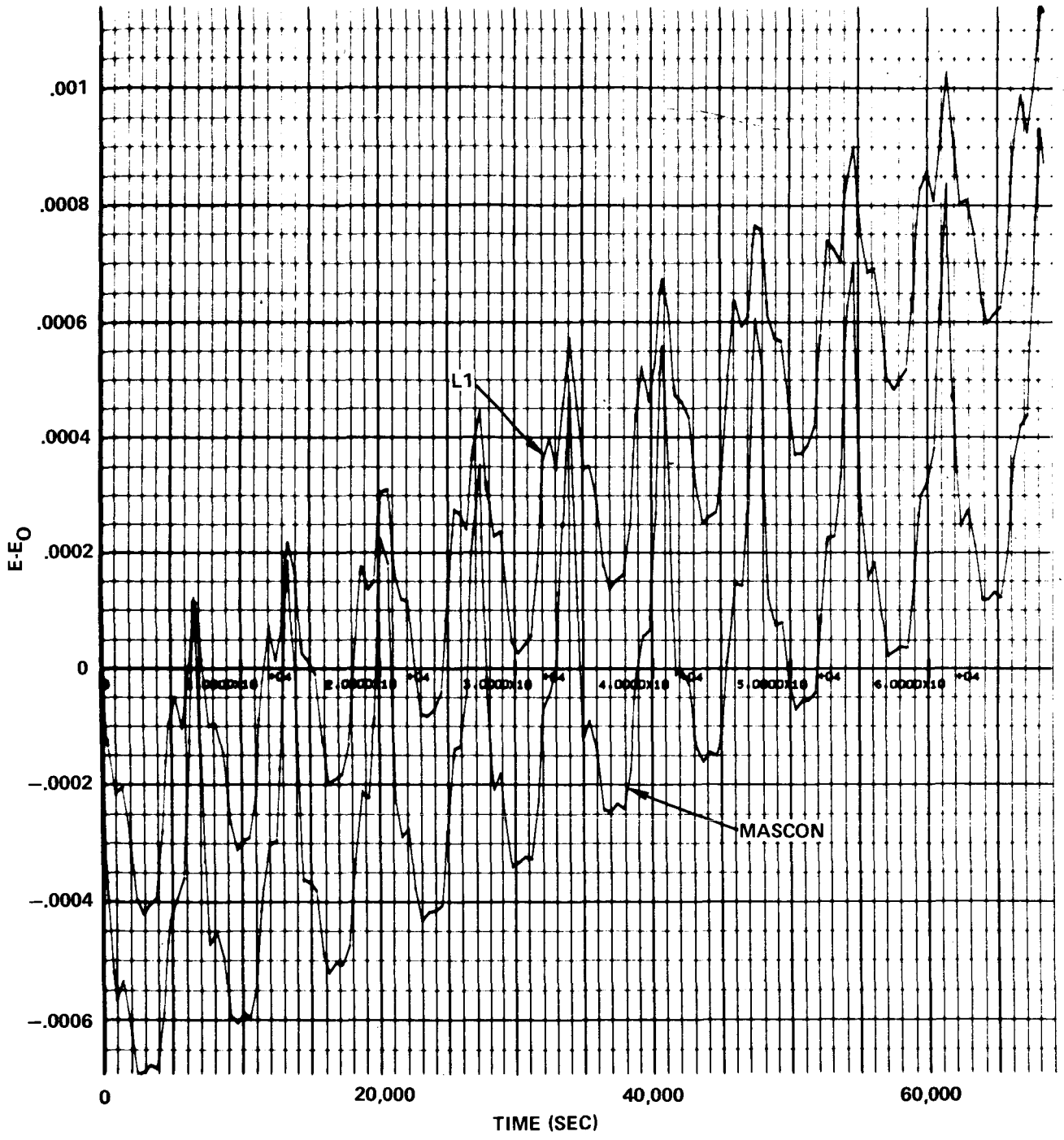

FIGURE 5 - ECCENTRICITIES (E_O = 0.025676294)

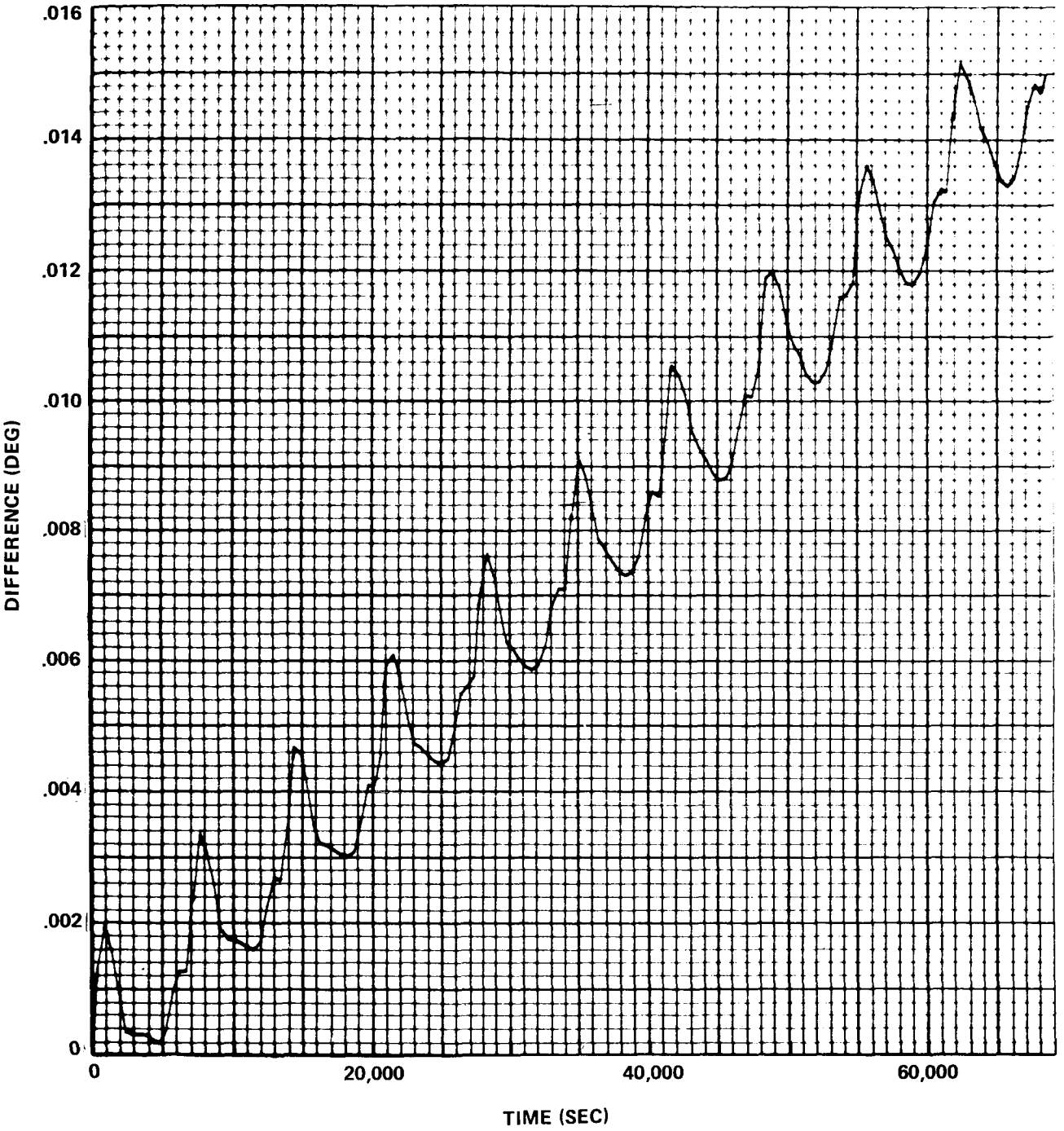

FIGURE 6 - INCLINATION DIFFERENCES

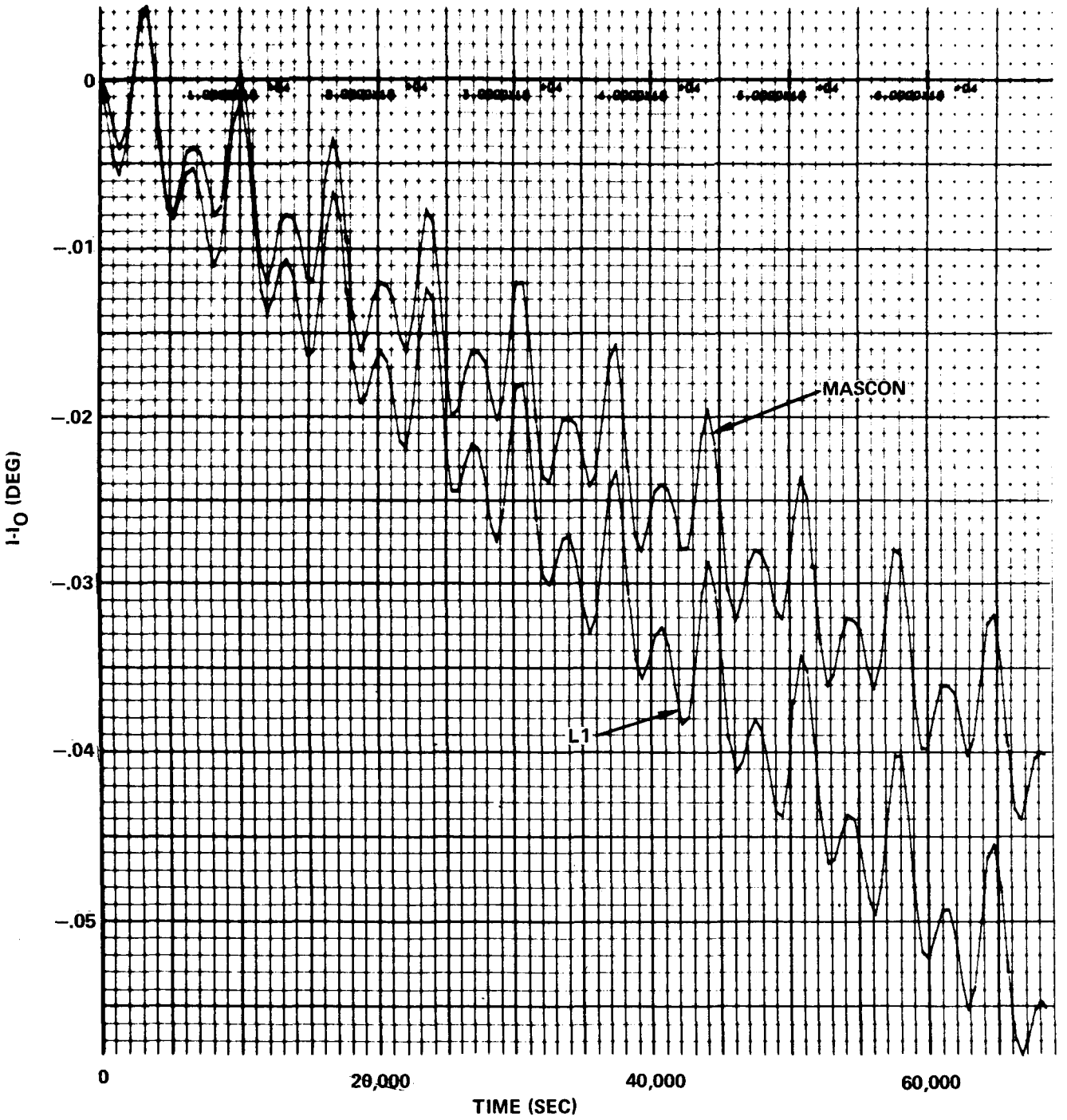

FIGURE 7 - INCLINATIONS (I_O = 153°.94926)

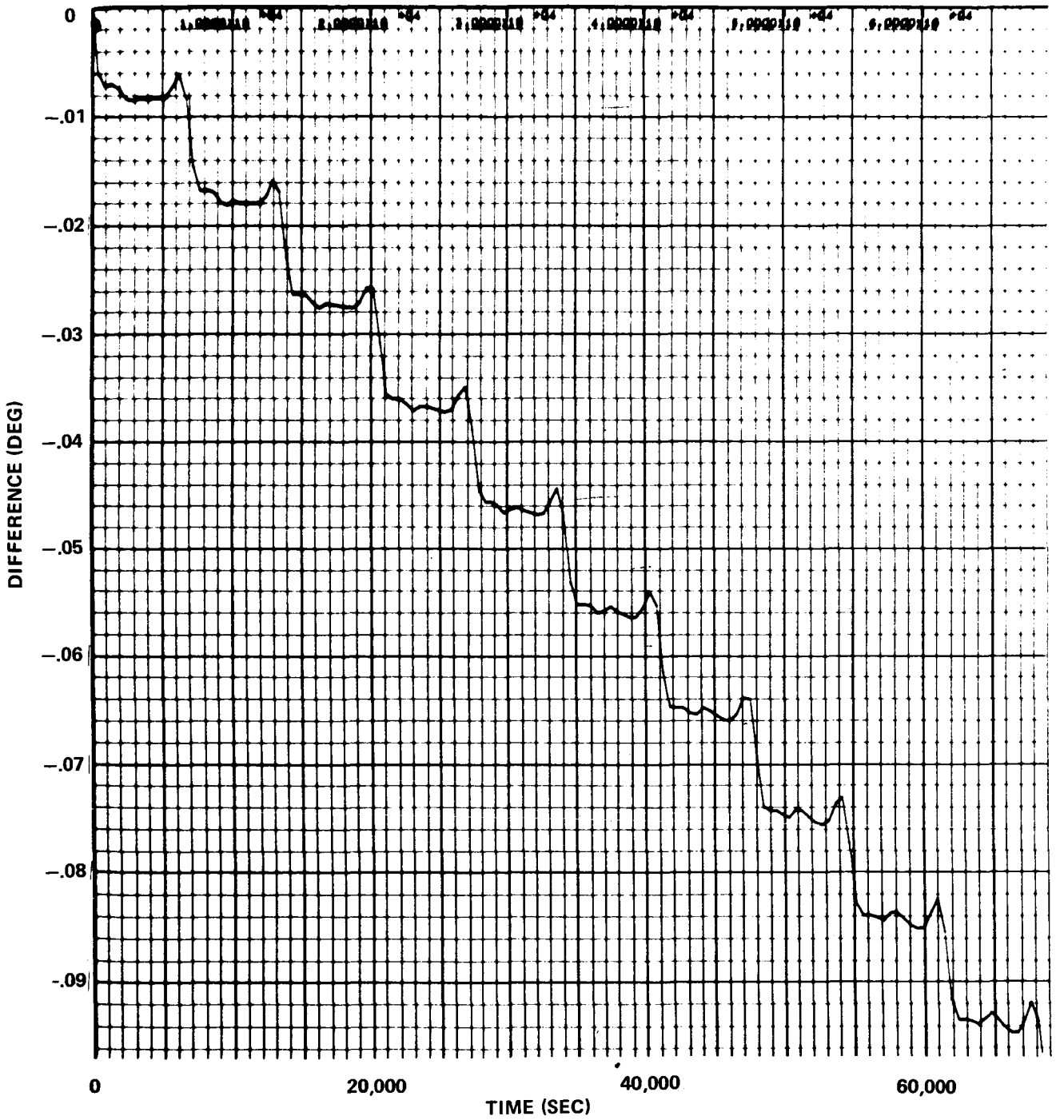

FIGURE 8 - INERTIAL NODE DIFFERENCES

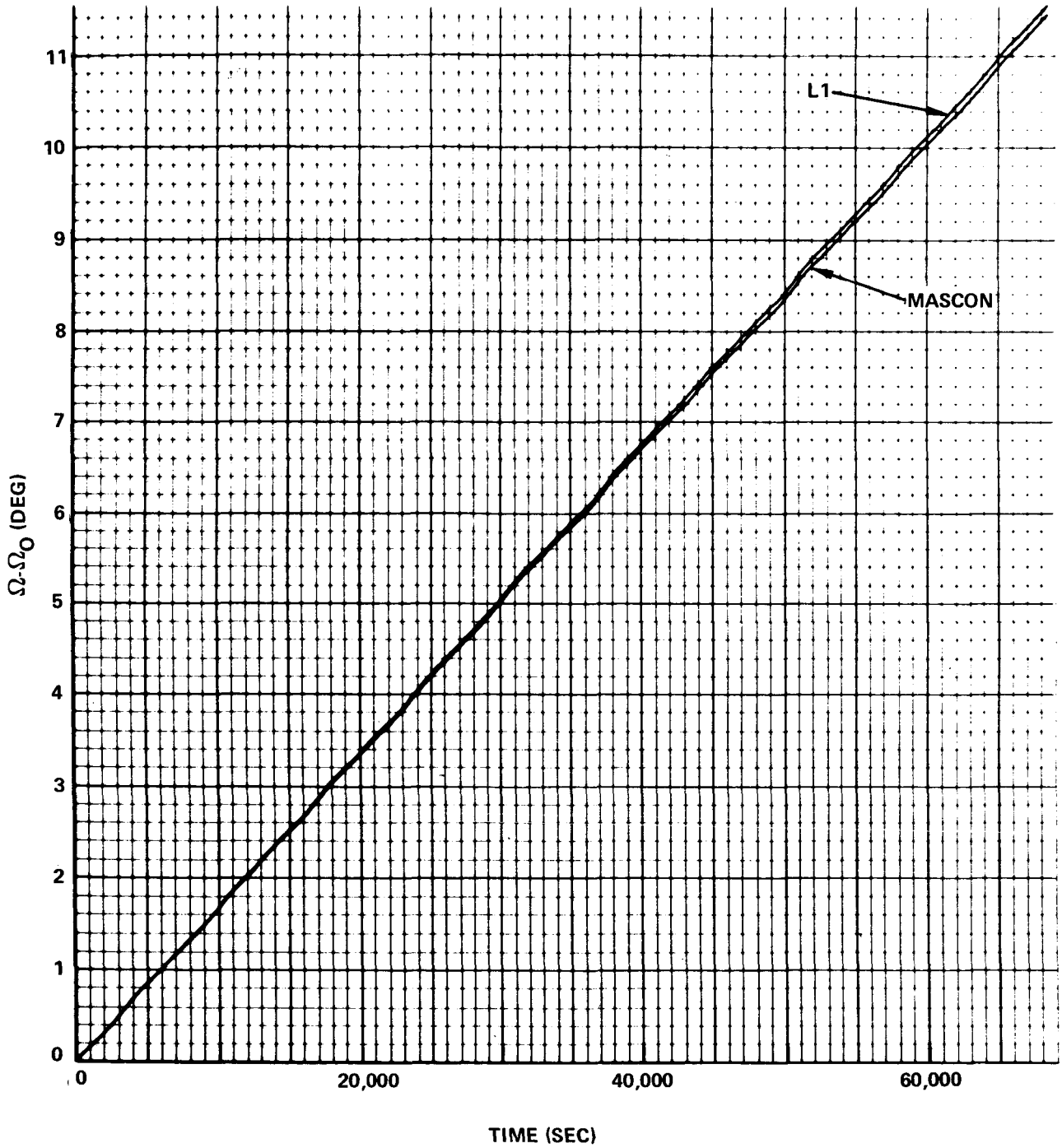

FIGURE 9 - INERTIAL NODES (Ω_O = 106°.12472)

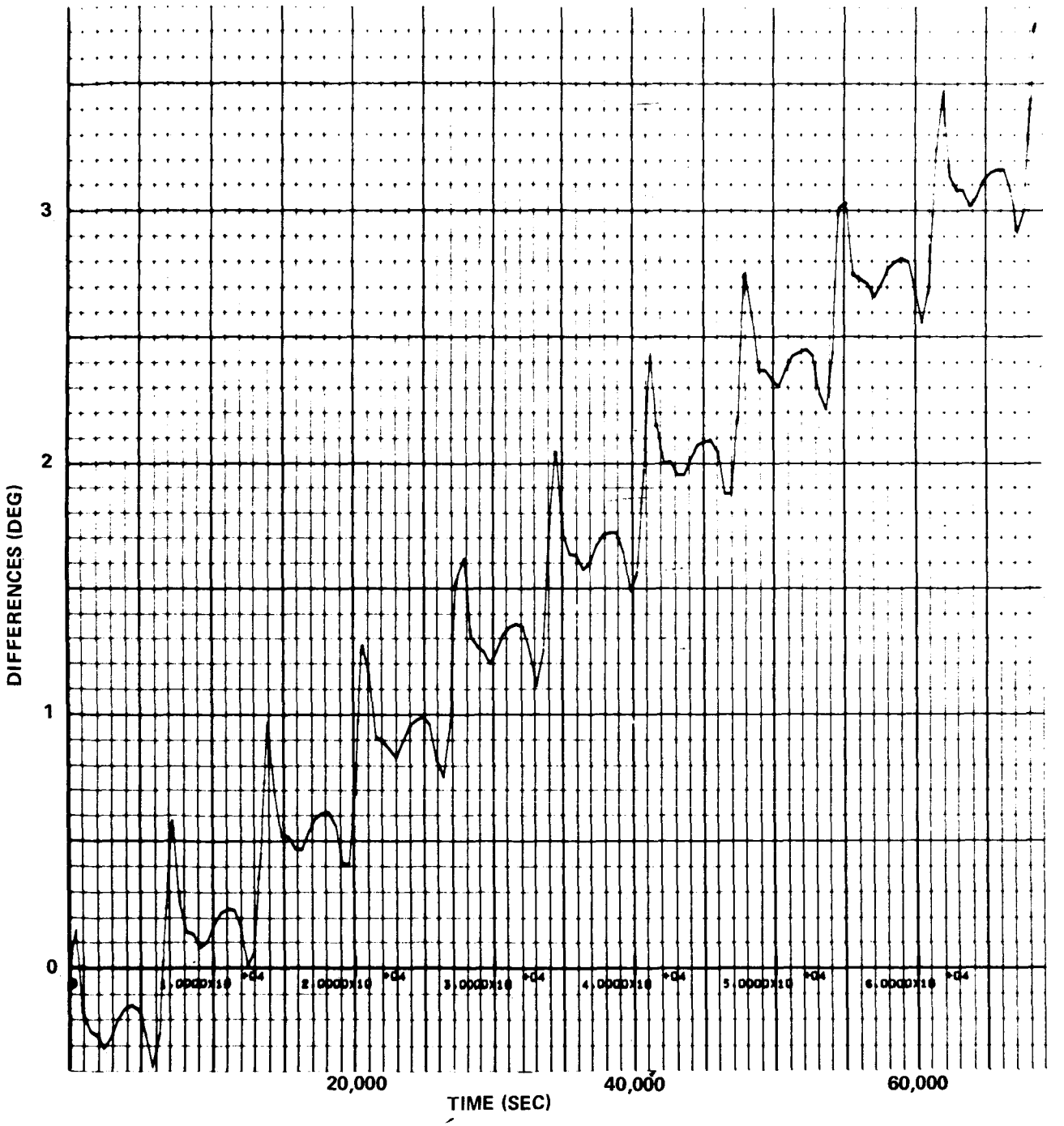

FIGURE 10 - DIFFERENCES IN ARGUMENT OF PERICENTER

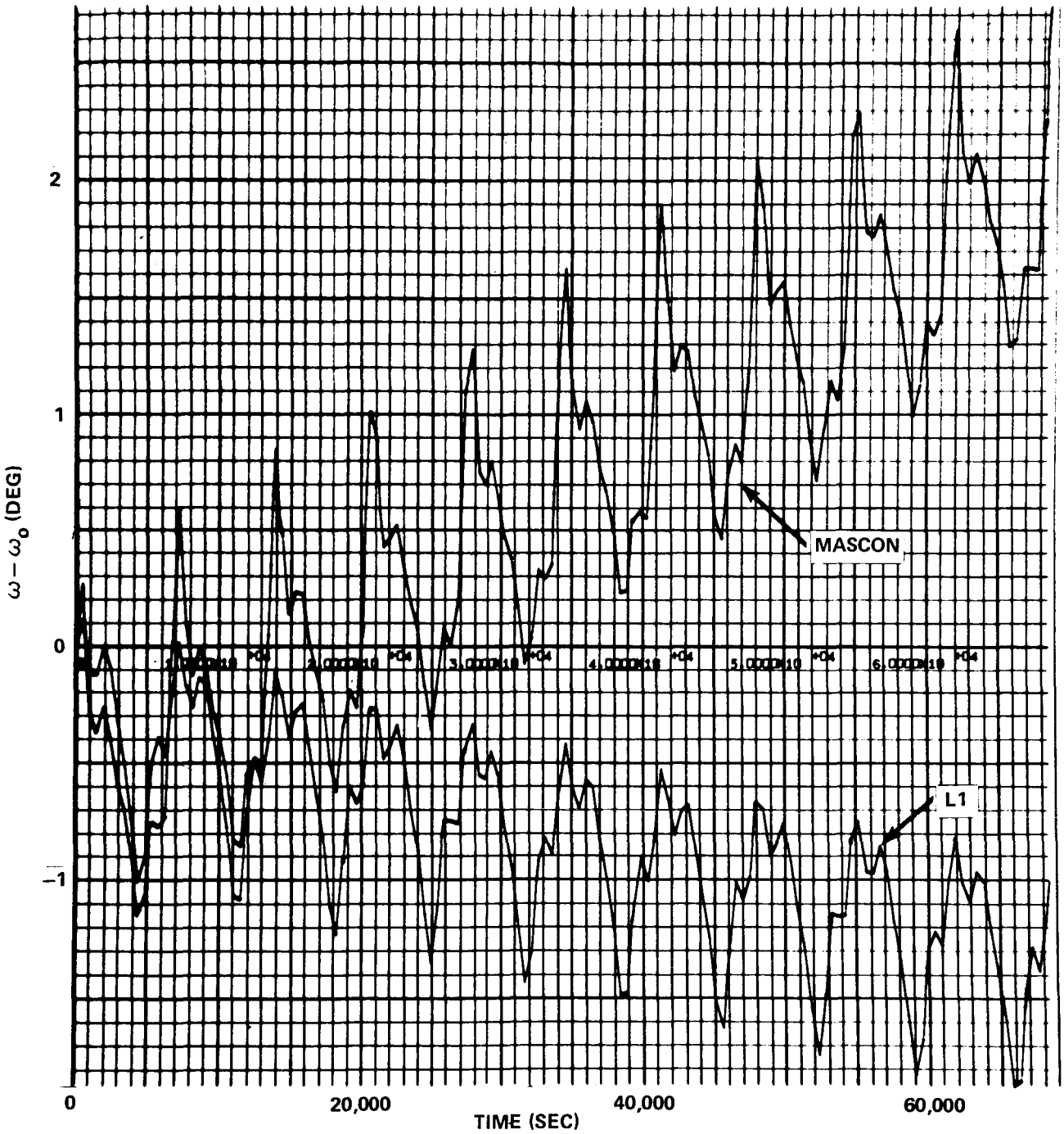

FIGURE 11 - ARGUMENTS OF PERICENTER (ω_o = 78°.582082)

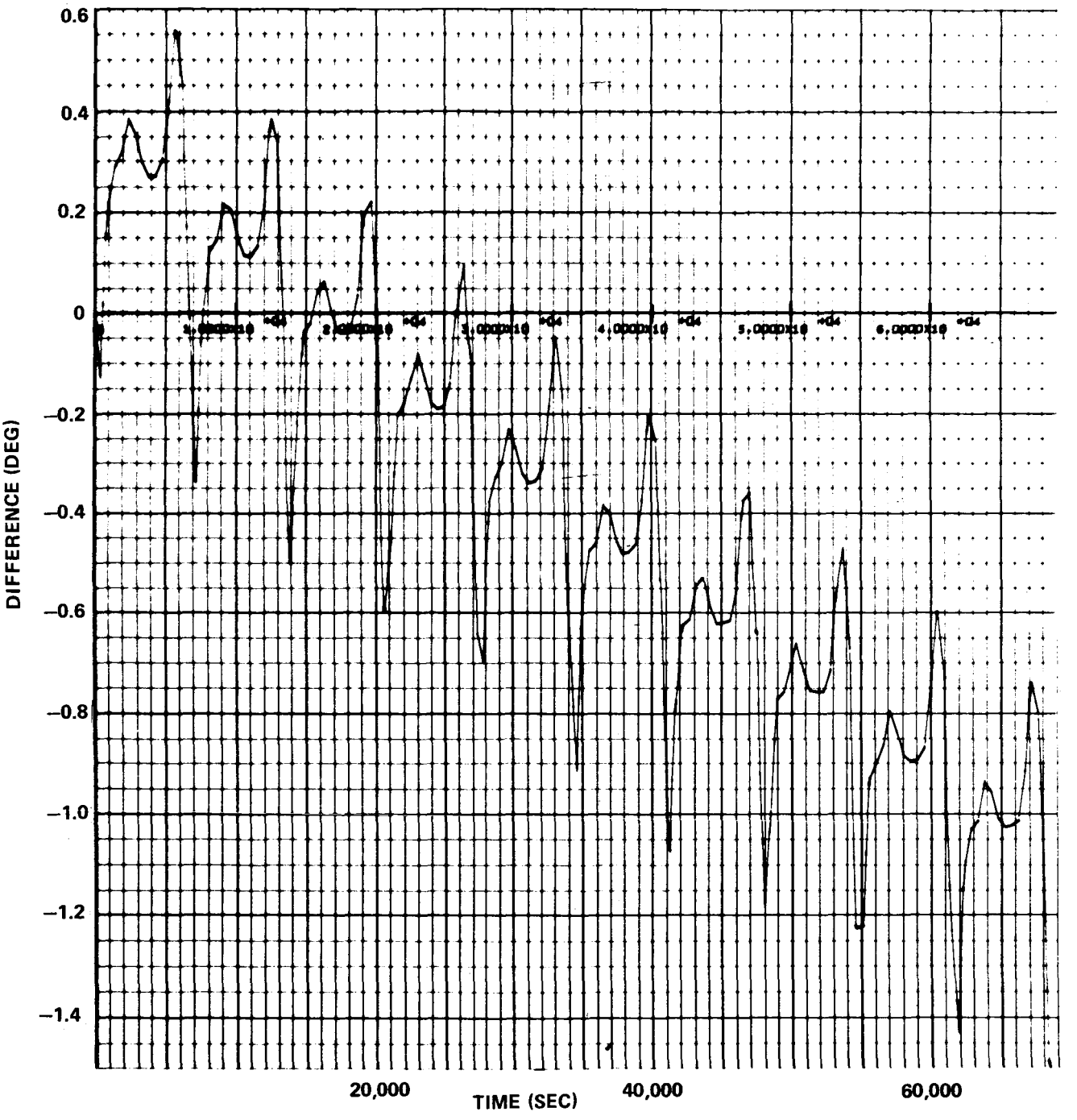

FIGURE 12 - MEAN ANOMALY DIFFERENCES

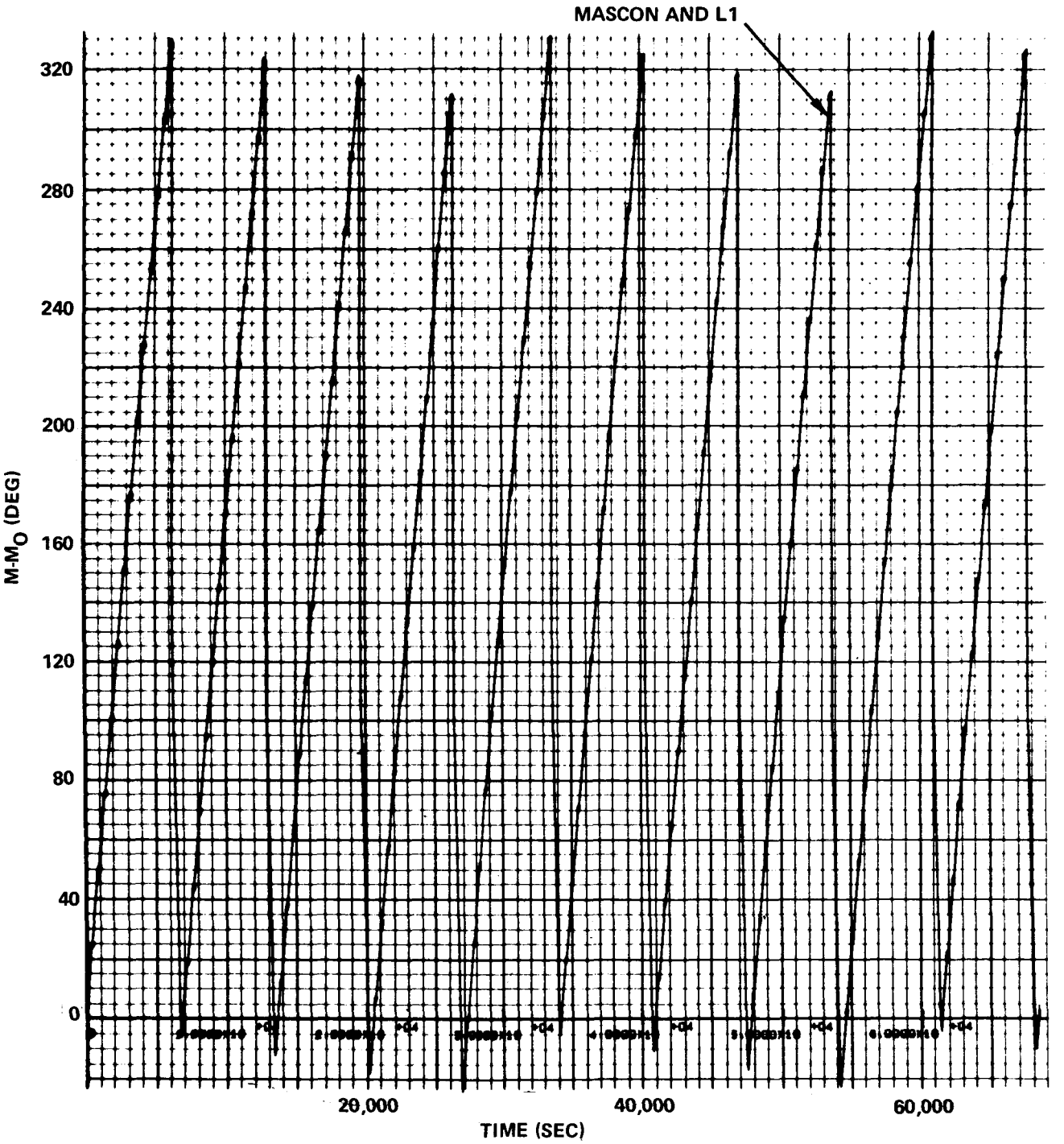

FIGURE 13 - MEAN ANOMALIES ($M_O = 25^\circ.02095$)

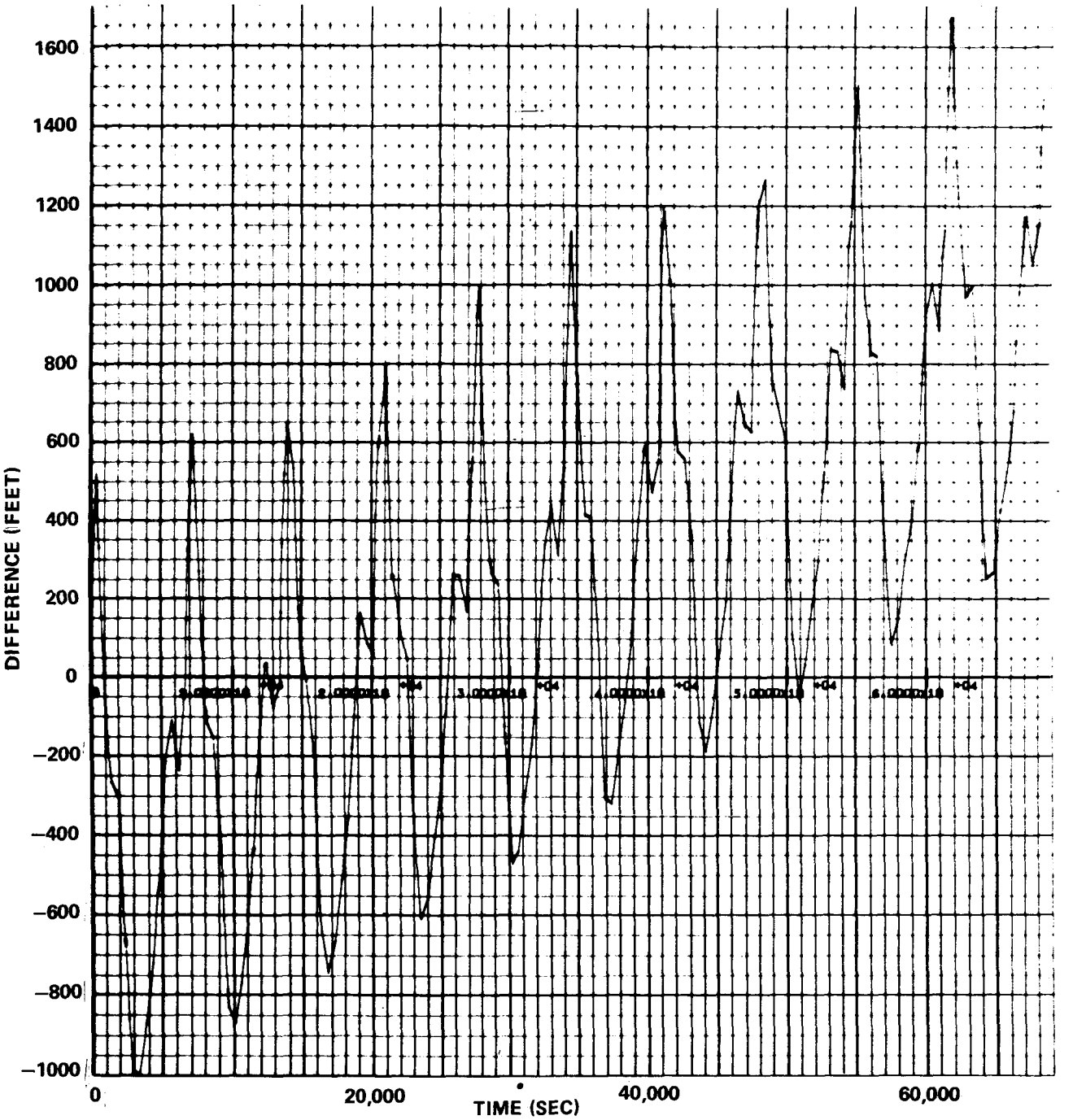

FIGURE 14 - PERILUNE ALTITUDE DIFFERENCES

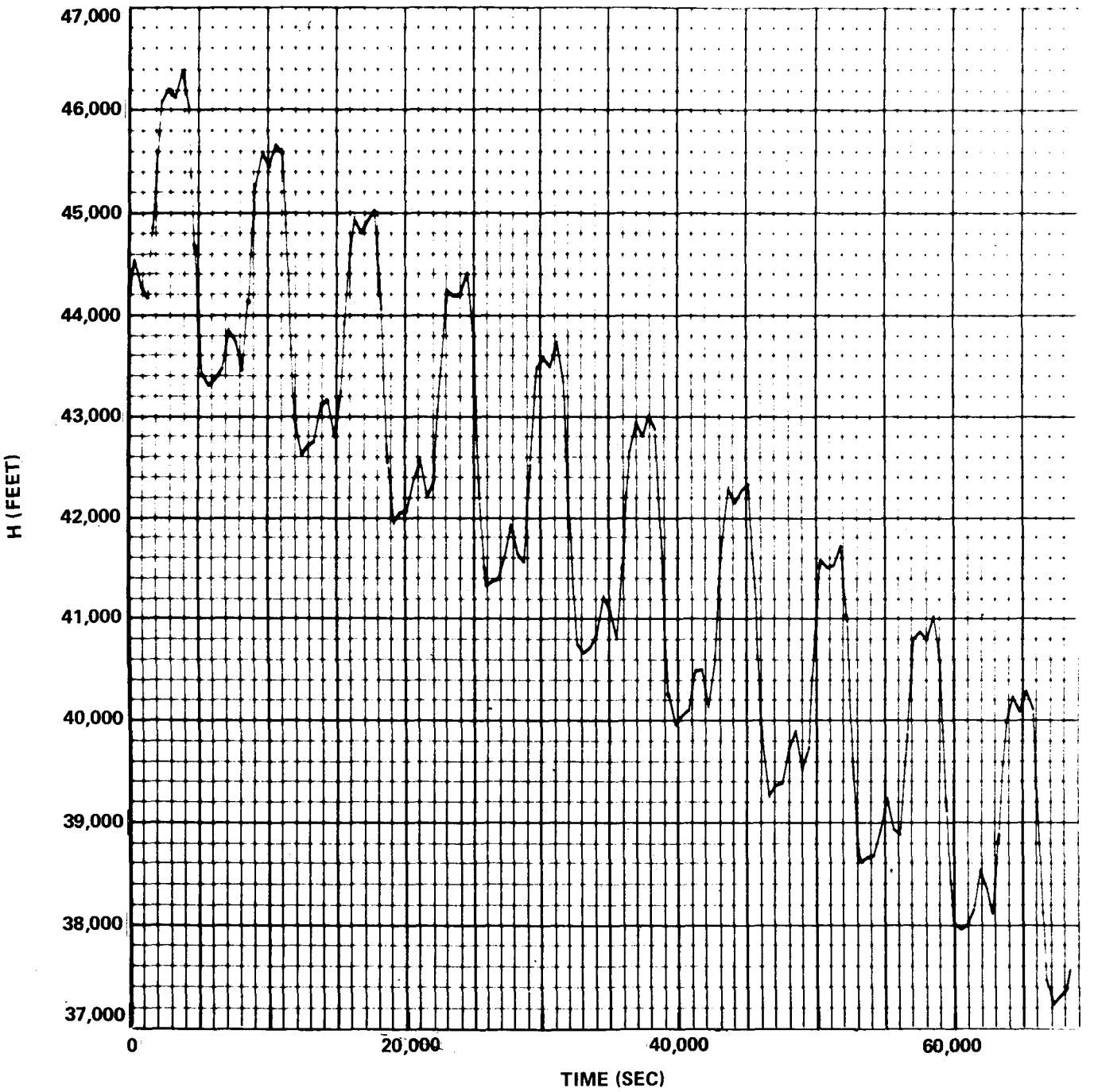

FIGURE 15 - PERILUNE ALTITUDE IN L1 POTENTIAL FIELD

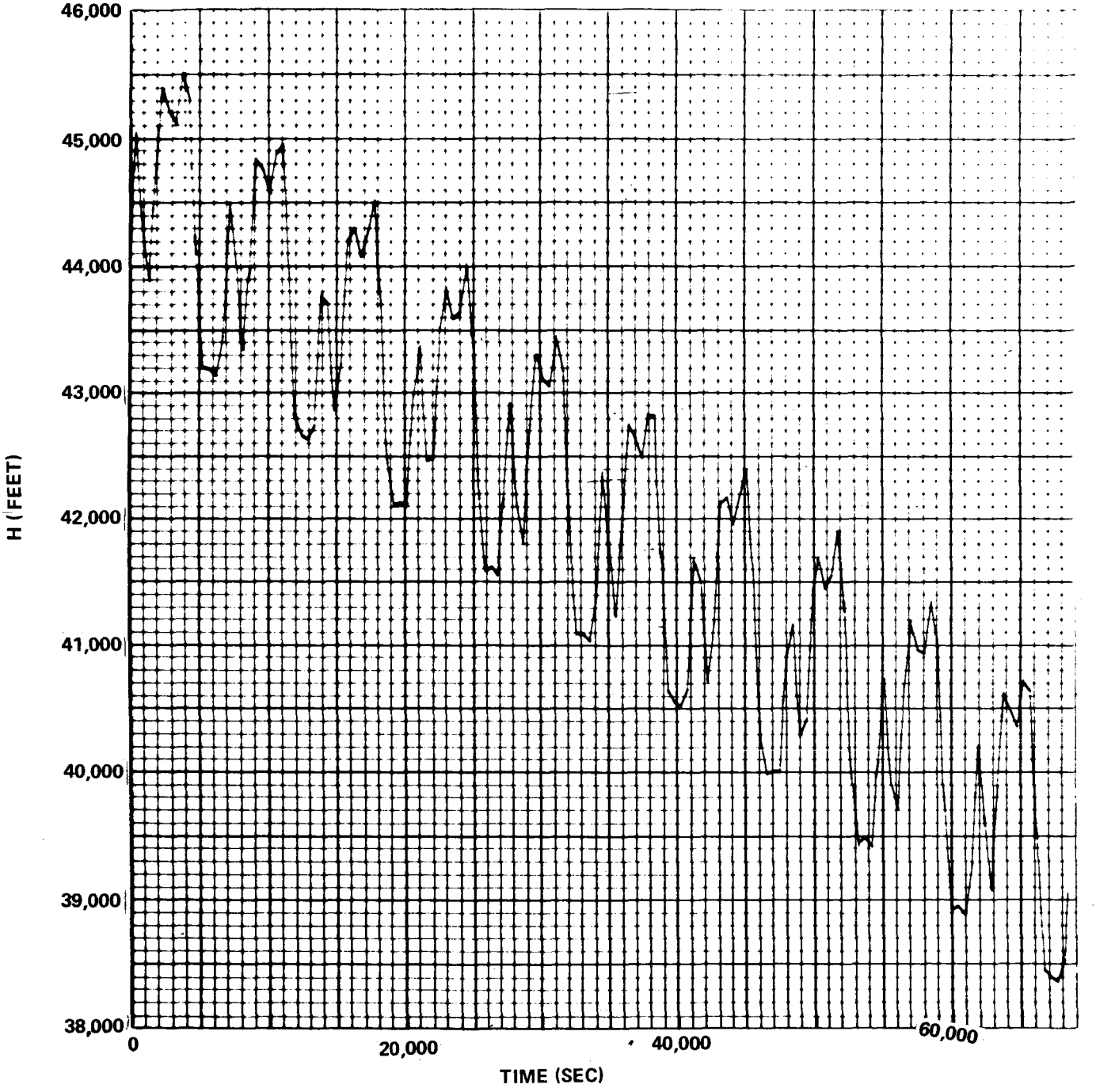

FIGURE 16 - PERILUNE ALTITUDE IN MASCON POTENTIAL FIELD

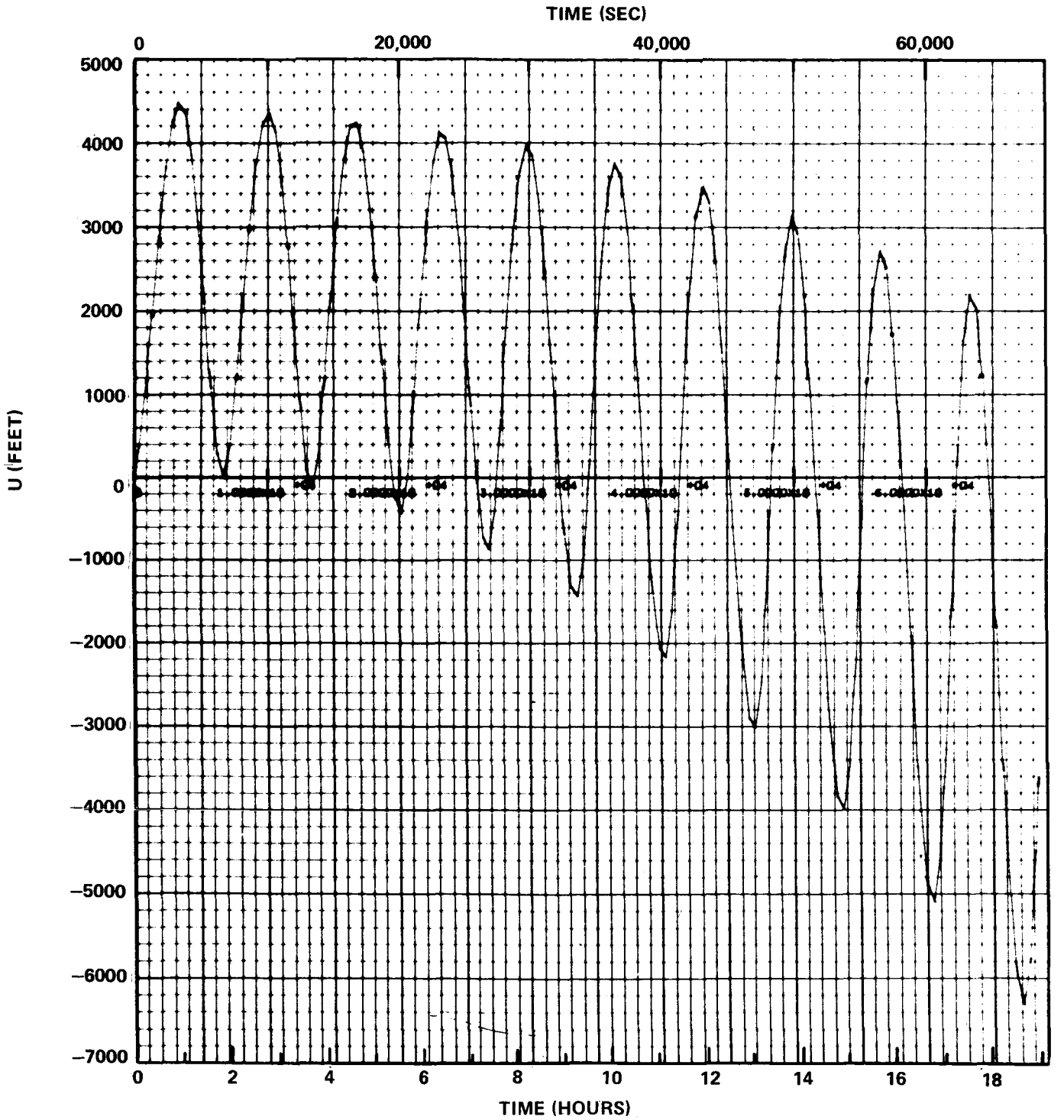

FIGURE 17 - VERTICAL ERRORS (U)

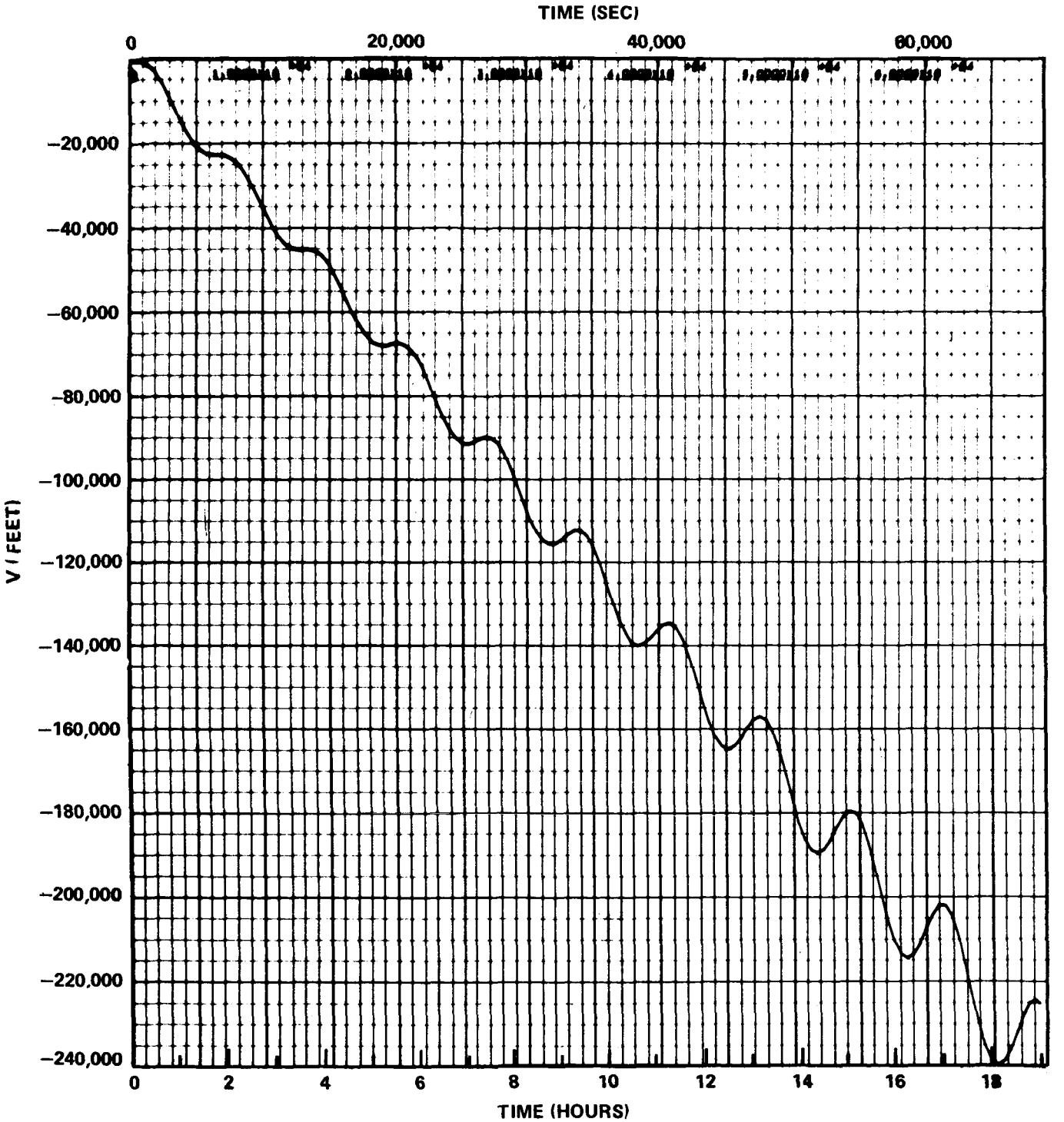

FIGURE 18 - DOWNRANGE ERRORS (V)

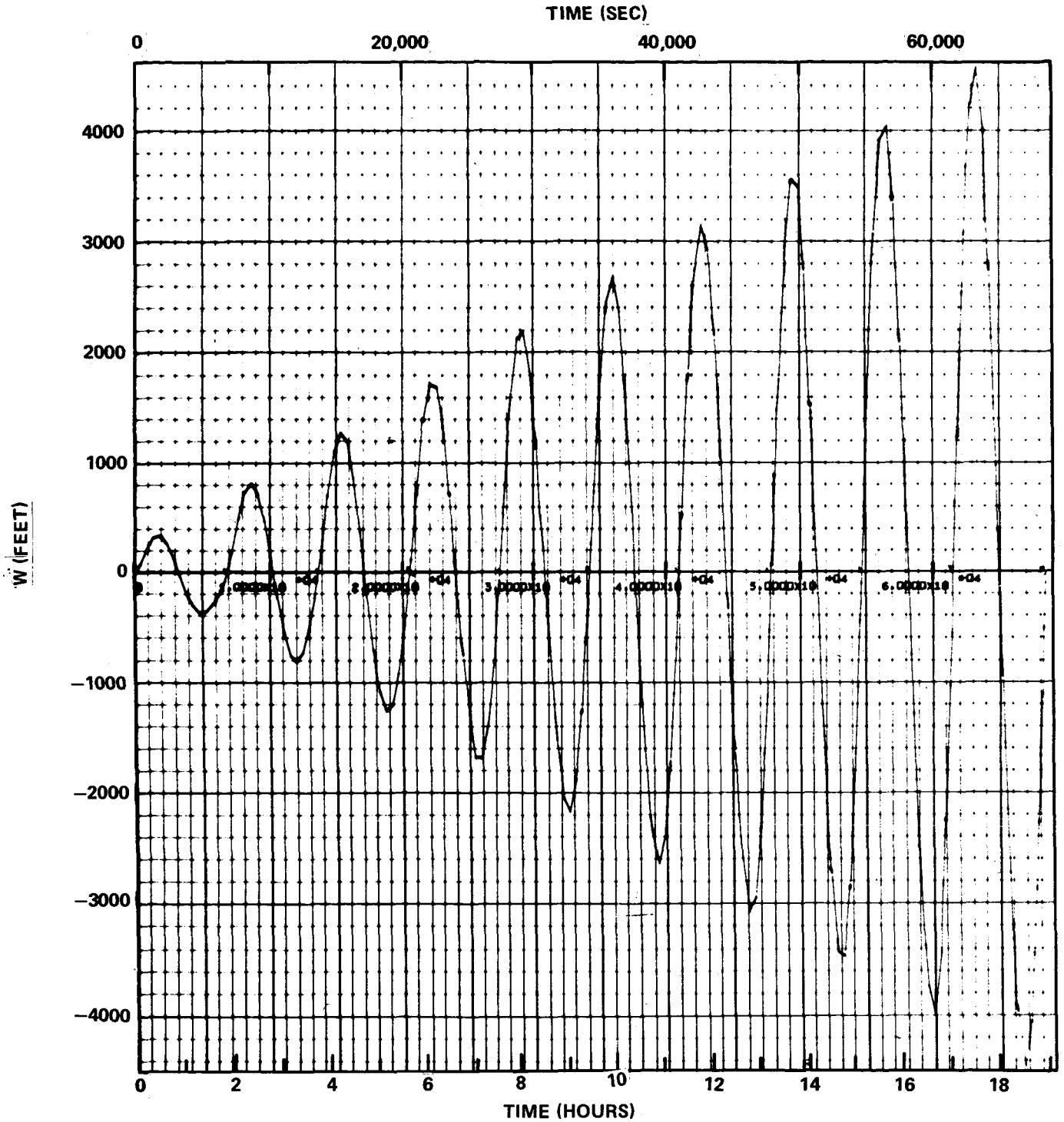

FIGURE 19 - CROSS TRACK ERRORS (W)

Subject: Possible Effects of Mascon Disturbances on Apollo 15 Orbit Determination and Navigation

From: S. L. Levie, Jr.

Distribution List

Complete Memorandum to

NASA Headquarters

J. K. Holcomb/MAO
E. W. Land, Jr./MAO
C. M. Lee/MA
A. S. Lyman/MR
W. E. Stoney/MAE

Manned Spacecraft Center

J. C. McPherson/FM4
R. K. Osburn/FM4
E. R. Schiesser/FM4
W. R. Wollenhaupt/FM4

Bellcomm, Inc.

R. A. Bass
A. P. Boysen, Jr.
M. V. Bullock
J. O. Cappellari, Jr.
D. A. De Graaf
F. El-Baz
W. W. Ennis
A. J. Ferrari
D. R. Hagner
W. G. Heffron
N. W. Hinners
T. B. Hoekstra
M. Liwshitz
J. L. Marshall
K. E. Martersteck
J. Z. Menard
P. E. Reynolds
R. V. Sperry
J. W. Timko
S. B. Watson
Department 1024 File
Central Files
Library

Abstract Only to

NASA Headquarters

R. A. Petrone/MA

Bellcomm, Inc.

J. P. Downs
D. P. Ling
M. P. Wilson